



HAL
open science

Design of selective divalent chain transfer agents for coordinative chain transfer polymerization of ethylene and its copolymerization with butadiene

Nicolas Baulu, Marie-Noëlle Poradowski, Ludmilla Verrieux, Julien Thuilliez, François Jean-Baptiste-Dit-Dominique, Lionel Perrin, Franck d'Agosto, Christophe Boisson

► To cite this version:

Nicolas Baulu, Marie-Noëlle Poradowski, Ludmilla Verrieux, Julien Thuilliez, François Jean-Baptiste-Dit-Dominique, et al.. Design of selective divalent chain transfer agents for coordinative chain transfer polymerization of ethylene and its copolymerization with butadiene. *Polymer Chemistry*, 2022, 13 (14), pp.1970-1977. 10.1039/D2PY00155A . hal-03721638v1

HAL Id: hal-03721638

<https://hal.science/hal-03721638v1>

Submitted on 1 Nov 2022 (v1), last revised 12 Jul 2022 (v2)

HAL is a multi-disciplinary open access archive for the deposit and dissemination of scientific research documents, whether they are published or not. The documents may come from teaching and research institutions in France or abroad, or from public or private research centers.

L'archive ouverte pluridisciplinaire **HAL**, est destinée au dépôt et à la diffusion de documents scientifiques de niveau recherche, publiés ou non, émanant des établissements d'enseignement et de recherche français ou étrangers, des laboratoires publics ou privés.

Design of selective divalent chain transfer agent for coordinative chain transfer polymerization of ethylene and its copolymerization with butadiene

Received 00th January 20xx,
Accepted 00th January 20xx

DOI: 10.1039/x0xx00000x

Nicolas Baulu,^{a,c,d} Marie-Noëlle Poradowski,^{b,c} Ludmilla Verrieux,^{b,d} François Jean-Baptiste-dit-Dominique,^{c,d} Lionel Perrin,^{*b,d} Franck D'Agosto,^{*a,d} and Christophe Boisson^{*a,d}

PhMg(CH₂)₅MgPh and MesMg(CH₂)₅MgMes – divalent bis metalated chain transfer agents (CTA) – were designed, synthesized and implemented in the polymerization of ethylene or the copolymerization of ethylene with butadiene mediated by $\{(\text{Me}_2\text{Si}(\text{C}_{13}\text{H}_8)_2)\text{Nd}(\mu\text{-BH}_4)[(\mu\text{-BH}_4)\text{Li}(\text{THF})]\}_2$. The systems showed coordinative chain transfer (co)polymerization features with a selectivity towards the initiation depending on the CTA used. Whereas PhMg(CH₂)₅MgPh initiated chain growth both at the alkyl and aryl sides, MesMg(CH₂)₅MgMes led to an unprecedented selective polymer chain growth from the alcanediyl moiety while the mesityl groups remain spectator. The mechanism of the polymerization initiation has been investigated computationnally at the DFT level. The theoretical contribution of the study highlights the different intermediates formed upon combination of the neodymium metallocene and the magnesium CTA, and rationalize the specificity conferred by the mesityl groups to the initiation for the production of telechelic polyolefins.

Keywords ethylene, butadiene, DFT, CCTP, telechelic, polymers

Introduction

Polyolefins account for more than half of the production of the produced plastics.¹ As they feature unique properties and are produced at a low price, polyolefins are ubiquitous in our daily lives. In the field of rubber materials, only few polymers are based on ethylene as a co-monomer although ethylene is highly available and can upon copolymerization confer high chemical resistance to the final product. For example, ethylene propylene rubber (EPR) and ethylene propylene diene monomer rubber (EPDM) are two classes of polyolefin-based rubber obtained by copolymerizing ethylene with α -olefins by coordination catalysis. Though the backbone of these polymers confers to the material interesting stability features, they are not used for tire applications. Styrene butadiene rubber (SBR), isoprene rubber (IR), butadiene rubber (BR) are indeed used in the tire industry.² In order to enlarge and/or shift material properties, there is a continuous need to develop new polyolefin rubbers. The copolymerization of olefins, including ethylene, with conjugated dienes has been one illustration of this challenging objective. This has been achieved by identifying the adequate catalysts³⁻¹² that produced copolymers combining the advantageous properties of olefins- and conjugated diene-based homopolymers.¹³

Among the catalysts reported, $\{(\text{Me}_2\text{Si}(\text{C}_{13}\text{H}_8)_2)\text{Nd}(\mu\text{-BH}_4)[(\mu\text{-BH}_4)\text{Li}(\text{THF})]\}_2$ (**1**) / BOMAG (BOMAG = *n*-butyl-*n*-

octylmagnesium) enabled the copolymerization of ethylene with butadiene and gave access to a new class of rubber called ethylene butadiene rubber (EBR).¹⁴ In this system, BOMAG acted both as an activator and a chain transfer agent (CTA). The resulting elastomers featured ethylene, *trans*-1,4, vinyl and 1,2-cyclohexyl units that are formed by intramolecular cyclization after a sequence of insertions of two ethylene units and a butadiene inserted in 2,1. Polymerization of ethylene or its copolymerization with butadiene mediated by this catalytic system have been shown to obey to a coordinative chain transfer (co)polymerization (CCTP).¹⁵ As a controlled polymerization technique, CCTP potentially allows the production of end-functional polyolefins,¹⁶⁻¹⁸ telechelic polyethylenes,¹⁹⁻²⁰ and block copolymers.²¹⁻²⁶ Employing a polymetalated CTA based on zinc, Lee et col. took the advantage of CCTP to control the copolymerization of ethylene with propylene using pyridylamido hafnium complexes.. The oxidation of the organozincs that are present on most of the chains allows a straightforward functionalization of both chain ends of the poly(ethylene-*co*-propene) elastomer produced. Alternatively, after turning the Zn centers into anionic polymerization initiator, styrene polymerization was further conducted leading to PS-*b*-poly(ethylene-*co*-propene)-*b*-PS triblock thermoplastic elastomers.^{23,26} However, the presence of terminal Zn-Et leads to parallel single chain growth providing a mixture of polymer chains. Recently, researchers at The Dow Chemical Company have reported the preparation of a divalent zinc CTA bearing a capping terminal group tailored for the selective synthesis of triblock copolymers polyethylene-*b*-poly(ethylene-*co*-octene)-*b*-polyethylene). In this approach, the preparation of the CTA involves a multistep procedure based on the use of several catalysts and requires the purification of the CTA.²⁷

In this context, it is of interest to develop simple and straightforward syntheses of divalent chain transfer agents that enable the controlled telechelic polymer chain growth. For that purpose, we have targeted the alcanediylmagnesium set of

^a Univ Lyon, Université Claude Bernard Lyon 1, CPE Lyon, CNRS, UMR 5128, Catalysis, Polymerization, Processes and Materials (CP2M), 43 Bd du 11 Novembre 1918, 69616 Villeurbanne, France

^b Univ Lyon, Université Claude Bernard Lyon I, CNRS, INSA, CPE, UMR 5246, ICBMS, 1 rue Victor Grignard, F-69622 Villeurbanne cedex, France

^c Manufacture Michelin, 23 places Carmes Déchaux, F-63000 Clermont-Ferrand, France

^d ChemistLab, Michelin CP2M ICBMS joint Laboratory 69616 Villeurbanne, France.

Electronic Supplementary Information (ESI) available: NMR analysis of polymers, NMR characterizations of CTA, computational speciation of CTA and Nd/CTA complexes aggregates. Cartesian coordinates and associated energies to all optimized structures. See DOI: 10.1039/x0xx00000x

compounds of the general formula $X\text{-Mg}(\text{CH}_2)_n\text{MgX}$ in which X has to be tolerated by $\{(\text{Me}_2\text{Si}(\text{C}_{13}\text{H}_8)_2)\text{Nd}(\mu\text{-BH}_4)[(\mu\text{-BH}_4)\text{Li}(\text{THF})]\}_2$ (**1**) and does not initiate polymerization. To achieve an efficient design of the CTA, a combined computational and experimental approach has been used. These bis-metalated divalent CTAs were designed to exclusively lead to telechelic polyethylene or poly(ethylene-co-butadiene) chains.

Experimental

General experimental information. All reactions involving air-sensitive compounds were carried out under a protective atmosphere of argon. The toluene used as solvent for the polymerization was purified on a SPS800 MBraun system. BOMAG 20 mol% solution in heptane was purchased from Chemtura. Deuterated solvents were supplied by Eurisotop. The bis(fluorenyl) neodymium complex was synthesized according to the literature.^{3,14,28} MeTHF was distilled over Na/benzophenone. 1,5-dibromopentane and 2-bromomesitylene (Sigma-Aldrich) were stored under molecular sieves. Butadiene and ethylene were supplied by Michelin and Air Liquide respectively.

NMR spectroscopy of organometallic complexes. The analyses were carried out on Bruker 400 and 500 Avance III spectrometers working at 400 MHz and 500 MHz for ^1H . The spectra were recorded with a 5 mm BBFO probe. The following program were used for 2D NMR: COSY: Pulse program; cosygppqf; SW: 11 ppm x 11 ppm; d1: 2 s; Impulsion 90° "hard" P1 = 13 μs and 16 W; Gradient: SMSQ10.100. HSQC: Pulse program; hsqcsetgps2; SW: 11 ppm (^1H) x 220 ppm (^{13}C); d1: 2 s; Impulsion 90° "hard" ^1H P1 = 13 μs and 16 W and ^{13}C P2 = 26 μs and 84 W; Gradient: SMSQ10.100. HMQC: Pulse program; hmqsetgp; SW: 11 ppm (^1H) x 220 ppm (^{13}C); d1: 1.47 s; Impulsion 90° "hard" ^1H P1 = 13 μs and 16 W and ^{13}C P2 = 26 μs and 84 W; Gradient: SMSQ10.100. HMBC: Pulse program; hmbcqnqdf; SW: 13.3 ppm (^1H) x 220 ppm (^{13}C); d1: 1.5 s; Impulsion 90° "hard" ^1H P1 = 13 μs and 16 W and ^{13}C P2 = 26 μs and 84 W; Gradient: SMSQ10.100. NOESY: Pulse program; noesygpphpp; SW: 9.6 ppm (^1H); d1: 1.98 s; Impulsion 90° "hard" P1 = 13 μs and 16 W; Gradient: SMSQ10.100.

NMR spectroscopy of polymers. Microstructures of the copolymers were determined by ^1H , ^{13}C NMR spectra recorded in TCE/ C_6D_6 mixture (volume ratio 2/1) at 363 K on a Bruker 400 Avance III spectrometer equipped with a 5 mm BBFO probe for ^1H and on a Bruker Avance II spectrometer equipped with a 10 mm PSEX probe for ^{13}C . The solutions were prepared at 1 wt% for ^1H and at 5 wt% for ^{13}C . Chemical shift values are referenced to the residual proton of deuterated benzene at 7.16 ppm for ^1H NMR and to the signal of TCE at 120.65 for ^{13}C NMR.

Size exclusion chromatography at high temperature. HT-SEC analyses were performed using a Viscotek system, from Malvern Instruments, equipped with three columns (PLgel Olexis 300 mm x 7 mm I.D.) from Agilent Technologies. Samples were dissolved in 1,2,4-TCB with a concentration of 3 mg mL⁻¹. 200 μL of sample solutions were injected and eluted in 1,2,4-TCB using a flow rate of 1 mL min⁻¹ at 150°C. 2,6-di-tert-butyl-4-

methylphenol (BHT) was added to the eluent (400 mg L⁻¹) to stabilize the polymer against oxidative degradation. Data were acquired and processed with the OmniSEC 5.02 software. Online detection was performed with a differential refractive index detector and a viscometer detector. A conventional calibration curve constructed with narrow polyethylene standards (M_p : 338 to 78400 g mol⁻¹) from Polymer Standards Service (Mainz, Germany) was used to calculate average molar masses of polyethylenes.

Size exclusion chromatography in THF. Measurements were performed with a Viscotek TDAmx system from Malvern Instruments that consists of a sample delivery module (GPCmax) including a four-capillary differential viscometer and a differential refractive index detector (RI). The separation was carried out on a guard column and three columns (SDVB, 5 μm , 300 x 7.5 mm I.D.) from Polymer Standard Service. THF was used as the mobile phase at a flow rate of 1 mL min⁻¹. Samples were dissolved in THF with a concentration of 3 mg mL⁻¹ and filtered on a PTFE membrane (0.45 μm). 100 μL of sample solutions were injected and eluted at a flow rate of 1 mL min⁻¹. Columns and detectors were maintained at 35°C. The OmniSEC 5.02 software was used for data acquisition and data processing. A universal calibration curve constructed with narrow polystyrene standards (M_p : 1306 to 2 520 000 g mol⁻¹) from Polymer Standards Service (Mainz, Germany) was used to calculate average molar masses.

Preparation of pentanediyl-1,5-di(mesitylmagnesium) MesMg(CH₂)₅MgMes. (i) *Solution of pentanediyl-1,5-di(magnesium bromide).* In a flask (50 mL) a suspension of magnesium (3.65 g, 6 equivalents) in 10 mL of MeTHF was activated by I₂ (20 mg). A solution of 1,5-dibromopentane (3.41 mL, 25 mmol) in 40 mL of MeTHF was added dropwise to this suspension under strong stirring. The temperature of the mixture was controlled between 35-40°C. The mixture is stirred during 16 hours. (ii) *Solution of 2-mesitylmagnesium bromide.* Magnesium (4.15 g, 3 equivalents) in 47.5 mL of MeTHF was activated by I₂ (20 mg). A solution of 2-bromomesitylene (7.65 mL, 50 mmol) and 2,5 mL of MeTHF was added dropwise to this suspension under strong stirring at 60°C. The mixture is stirred at 60°C for 3h and then at room temperature for 16 hours. (iii) *Solution of pentanediyl-1,5-di(mesitylmagnesium).* Solutions from experiments (i) and (ii) were combined. A solution of 1,4-dioxane (10.3 mL, 120 mmol) in 20 mL of MeTHF was added dropwise to the mixture. A white precipitate is rapidly observed, and the suspension was stirred during 20 h before being filtered off under celite. The solvent is evaporated leading to an oily product (17.88 g). The ^1H NMR of the product in C_6D_6 showed a ratio MeTHF/Mg of 2.6.

The product was solubilized in toluene to obtain a concentration of 0.45 M. This solution was used for the polymerization tests. ^1H NMR of the oil (C_6D_6 – 298 K). δ : ppm = 6.98 (s, 4H, f, H-Mes), 2.63 (s, 12 H, d, Me), 2.36 (s, 6H, e, Me), 2.21 (quin, 4H, Mg-CH₂-CH₂), 1.95 (quin, 2H, Mg-CH₂-CH₂-CH₂), 0.12 (t, 4H, Mg-CH₂).

Typical polymerization protocol. Polymerizations were performed in a 250 mL glass reactor, equipped with a stainless-steel blade. The CTA and the neodymium complex were

introduced in a flask containing 200 mL of toluene. The mixture was stirred for 10 min and then transferred into the reactor under a stream of argon. Argon was then pumped out, and the reactor was charged with a mixture of butadiene and ethylene. The pressure is then gradually increased to 4 bars at the same time as the desired temperature is reached and kept constant during the entire reaction. Once the polymerization is complete, the reactor is cooled and degassed. The polymer was then precipitated in 400 mL of methanol, washed, and dried at 70°C under vacuum.

Computational details. The B3PW91^{29,30} hybrid functional is used with a single-point dispersion correction performed at the D3-BJ level.^{31,32} Bulk solvation by toluene is modelled by an implicit solvent model (SMD = toluene).³³ Coordination by co-solvent molecules has been explicitly considered in the chemical model. Hydrogen, carbon, and oxygen atoms are represented by polarized Pople bases triple- ζ valences (6-311(*d,p*)).³⁴ Magnesium is represented by the same type of basis set augmented by a diffuse function (6-311++(*d,p*)).^{34,35} For silicon, the quasi-relativistic pseudo-potentials of Stuttgart-Dresden-Bonn and its associated base augmented by a *d* polarization function ($\zeta_d(\text{Si}) = 0.284$) has been used.³⁶ Neodymium has been described also by a large core quasi-relativistic Stuttgart-Dresden-Bonn pseudo-potential (49-electron) and its associated basis set augmented by a *f* function ($\zeta_f(\text{Nd}) = 1.0$).^{37,38} All calculations have been realized without any symmetry restrictions using Gaussian 09 suite of programs.³⁹ The nature of the extrema (minimum and transition state) has been verified by analytical frequency calculations. Gibbs free energy values are estimated at 298 K and 1 atm and computed within the harmonic approximation. Conformational sampling and speciation of organometallic aggregates have been performed by hand. The Non-Covalent Interaction analyses have been performed using NCIPLLOT.⁴⁰

Results and discussion

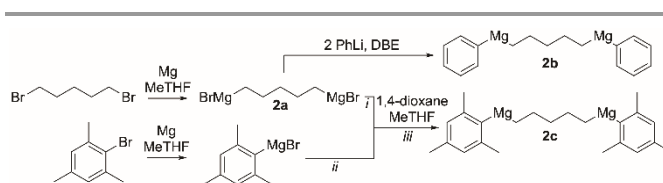
Proof of concept, design of $\text{PhMg}(\text{CH}_2)_5\text{MgPh}$. To derive profit from a significant difference of reactivity between Nd-C(alkyl) vs Nd-X bonds towards olefin insertion, we have considered X = Ph as a first guess. For that purpose, the homopolymerization of ethylene was implemented in the presence of **1** and MgPh_2 (Table 1, run 1). A rapid precipitation was observed at 70°C. Assuming a CCTP process, this was not consistent with the low theoretical number average molar mass targeted ($M_n = 1670 \text{ g mol}^{-1}$) and supports the low efficiency of MgPh_2 in promoting a controlled CCTP of ethylene. While NMR analyses of the obtained polymer confirmed that initiation does take place at the Nd-Ph site (Figure S1), the polymerization is indeed not controlled since the PE produced display a M_n of 8200 g mol^{-1} that is much higher than expected one of 1670 g mol^{-1} . Considering the M_n obtained and the amount of MgPh_2 used, only 0.4 PE chains are initiated. The poor initiation efficiency of phenyl groups and the good CCTP control conferred by dialkylmagnesium (e.g. BOMAG) to ethylene polymerization performed under similar conditions⁴¹ led us to consider

$\text{PhMg}(\text{CH}_2)_5\text{MgPh}$ (**2b**, Scheme 1) as CTA in combination with complex **1**.

The preparation of alcanediyl magnesium compounds appears more straightforward than zinc counterparts depicted in literature that require boron/zinc²³ or magnesium/zinc⁴² transmetalation steps. Access to $\text{PhMg}(\text{CH}_2)_5\text{MgPh}$ (**2b**) is afforded from di(magnesium bromide)pentanediyl ($\text{BrMg}(\text{CH}_2)_5\text{MgBr}$, **2a**) Grignard reagent that is classically synthesized by reacting dibromopentane with magnesium in 2-methyltetrahydrofuran (MeTHF). $\text{PhMg}(\text{CH}_2)_5\text{MgPh}$ (**2b**) is then obtained by transmetalation between freshly prepared $\text{BrMg}(\text{CH}_2)_5\text{MgBr}$ (**2a**) and 2 equivalents of PhLi. The awaited reagent **2b** is ultimately obtained in solution in toluene solution at a concentration of 0.37 M. The NMR analysis of **2b** confirmed the presence of two phenyl groups per pentanediyl group (Figure S2) in agreement with the structure targeted.

Polymerization of ethylene was then performed using $\{(\text{Me}_2\text{Si}(\text{C}_{13}\text{H}_8)_2)\text{Nd}(\mu\text{-BH}_4)[(\mu\text{-BH}_4)\text{Li}(\text{THF})]\}_2$ in combination with **2b** as CTA. The ^1H NMR analysis of the obtained polymer reveals that polyethylene chains are initiated both at the alkyl and aryl sites of the CTA (Figure S3). Consequently, the average molar mass is lower than the one expected if initiation would have specifically occurred at the alcanediyl moiety. More quantitatively, as 54% of the polymer chains are initiated by a phenyl group, the transmetalation step between the CTA and the Nd complex required to initiate the polymerization is not chemoselective enough towards alcanediyl moiety to ensure a quantitative initiation from this group. The ability of alcanediylmagnesium **2b** to initiate and act as a CTA for the copolymerization of ethylene with butadiene was also assessed (Table 1, run 3). The copolymerization did proceed but the activity of the catalysts is lower ($27 \text{ g mol}^{-1} \text{ h}^{-1}$) than that generally measured using BOMAG as CTA ($150 \text{ g mol}^{-1} \text{ h}^{-1}$, Table 2, run 6).

The microstructure of the obtained copolymer is in line with the one expected for copolymers synthesized under similar conditions with BOMAG (Table 3) and the molar mass (6940 g mol^{-1}) is in good agreement with that calculated considering an initiation of one polymer chain per CTA (7230 g mol^{-1}). As in the case of ethylene homopolymerization, the ^1H NMR analysis of the copolymer reveals nevertheless that some chains originate from initiation at a Nd-Ph site (Figure S4). A better chemoselectivity of initiation at the alcanediyl moiety seems thus to be obtained when copolymerizing ethylene and butadiene. Still, the selectivity of bis-metaleo CTA (**2b**) towards needs to be further improved to afford a quantitative formation of telechelic copolymer chains. For that purpose, molecular modelling and reaction pathways exploration have been performed at the DFT level.



Scheme 1 General procedure for the preparation of $\text{PhMg}(\text{CH}_2)_5\text{MgPh}$ (**2b**) and $\text{MesMg}(\text{CH}_2)_5\text{MgMes}$ (**2c**)

Table 1 Polymerization of ethylene and butadiene with the catalysts **1**/PhMg(CH₂)₅MgPh

Run ^a	Polymer ([E]/[B] in feed)	[Mg]/[Nd]	Yield (g)	Polymerization time (min)	Activity (g mol ⁻¹ h ⁻¹)	<i>M_n</i> ^{theo c} (g mol ⁻¹)	<i>M_n</i> (Đ) ^d (g mol ⁻¹)
1 ^b	PE	69	5.40	60	230	1670	8200 (1.9)
2	PE	30	5.50	18	367	7430	4400 (1.4)
3	EBR (80/20)	30	5.35	235	27	7230	6940 (1.5)

^a Conditions: 200 mL of toluene, 3.5 bar, 70°C, [Nd] = 250 μM. ^b [Nd] = 59 μM, CTA = MgPh₂. ^c *M_n*^{theo} = yield/*n*_{chain} with *n*_{chain} = 2 *n*(MgPh₂) or *n*(PhMg(CH₂)₅MgPh). ^d HT SEC in 1,2,4-trichlorobenzene for PE and in THF at 35°C for EBR.

Table 2 Polymerization of ethylene and butadiene with the catalysts **1**/MesMg(CH₂)₅MgMes

Run ^a	Polymer ([E]/[B] in feed)	[Nd] (μM)	[Mg]/[Nd]	Yield (g)	Polymerization time (min)	Activity (g mol ⁻¹ h ⁻¹)	<i>M_n</i> ^{theo e} (g mol ⁻¹)	<i>M_n</i> (Đ) ^f (g mol ⁻¹)
4 ^b	PE	62	145	1.38	19	315	1390	1640 (1.5)
5 ^c	PE	78	231	2.03	46	172	1130	940 (1.4)
6 ^d	EBR (80/20)	250	10	12.0	96	150	12000	15400 (1.3)
7	EBR (80/20)	250	10	10.6	86	148	42400	33100 (1.3)
8	EBR (80/20)	250	20	10.3	112	110	20600	18000 (1.3)
9	EBR (80/20)	250	40	10.5	145	87	10500	9800 (1.3)

^a Conditions: 200 mL of toluene, 3.5 bar, 70°C. ^b The polymerization was deactivated with iodine. ^c The polymerization was deactivated with MeOD. ^d BOMAG. ^e *M_n*^{theo} = yield/*n*_{chain} with *n*_{chain} = 2 *n*(BOMAG) or *n*(MesMg(CH₂)₅MgMes). ^f HT SEC in 1,2,4-trichlorobenzene for PE and in THF at 35°C for EBR.

Table 3 Microstructure of ethylene/butadiene copolymers^a

Run ^b	ethylene	<i>trans</i> -1,4	vinyl	1,2-cyclohexyl
3	73.0	6.5	10.7	9.8
6	75.5	5.5	9.4	9.6
7	73.3	6.3	11.0	9.3
8	73.8	6.1	10.8	9.3
9	75.3	5.6	9.4	9.7

^a Determined by NMR. ^b Conditions: 200 mL of toluene, 3.5 bar, 70°C.

Molecular modelling, in silico-based optimization. To rationally guide the design of the targeted bis-metated CTA, the mechanism of the initiation step of ethylene polymerization has been investigated computationally at the DFT level. The aim of this modelling section is to assess initiation selectivity trends depending on the nature of the group transferred to the Nd center. For this mechanistic investigation, the alkylated / arylated form of the pre-catalyst **1** has been considered. Firstly, to establish a common energy reference associated to the most stable structures, the speciation of each species has been performed (Figure S13). As the pentanediyli moiety of the bimetallic compound **2b** contains two symmetrical metated active sites, it has been modelled by a monometallic compound in which the pentanediyli group is replaced by a *n*-butyl group. The 2-Me-THF (MeTHF) used experimentally as a co-solvent has been explicitly considered in the chemical model. Bulk solvation by toluene has been described implicitly by a continuum model. In this microsolvation approach, four molecules of MeTHF have been represented to account for the experimental Mg / MeTHF stoichiometry. In a previous study, we have shown that addition of ether (nBu₂O) as a cosolvent to toluene solution of nBu₂Mg leads to the dissociation of high order aggregates into dimers in which one ether solvent molecule is coordinated on each magnesium.⁴¹ Similarly, in the present study, the most stable organomagnesium clusters magnesium dimers in which one

MeTHF solvent molecule is bonded to each Mg centre are: (σ-MeTHF)(σ-Ph)Mg(μ-*n*Bu)2Mg(σ-MeTHF)(σ-Ph) and (σ-MeTHF)(σ-*n*Bu)Mg(μ-*n*Bu)(μ-Ph)Mg(σ-MeTHF)(σ-Ph), these two structures can be considered as isoenergetic.

Concerning the Nd/Mg heterobimetallic complexes, the most stable complex is the heterotrimer complex {(Me₂Si(C₁₃H₈)₂)Nd(μ-*n*Bu)₂Mg(μ-Ph)₂Mg(σ-*n*Bu)·MeTHF} (**3**) in which one MeTHF is bonded to the terminal magnesium centre. In the following, complex **3** will be considered as the most stable dormant species (Figure S13) and its energy will be taken as the reference point, along with the separated organic molecules needed to define the chemical equilibria investigated in the energy profiles presented hereafter.

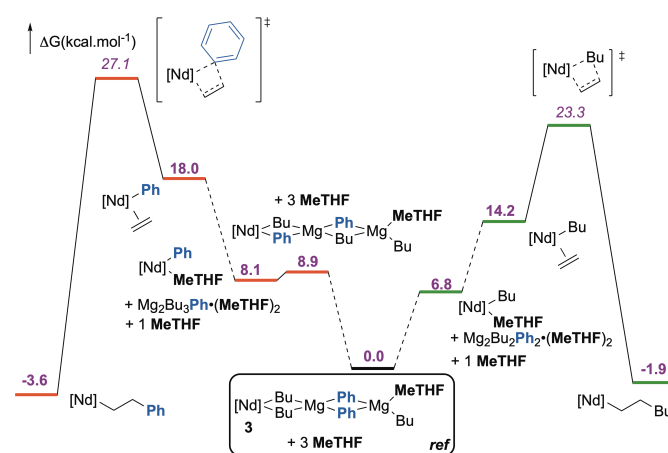


Figure 1 Gibbs free energy profile for the initiation of ethylene polymerization mediated by the [Nd]Bu/BuMgPh model system. Green (resp. red) pathways correspond to the initiation in an alkyl (resp. phenyl) site. Energies referring to kinetics are in italic, energies referring to thermodynamics are in bold. [Nd] correspond to [(Me₂Si(C₁₃H₈)₂)Nd]. ΔG in kcal mol⁻¹ (B3PW91, TZVP, SMD(Toluene), D3BJ(SP))

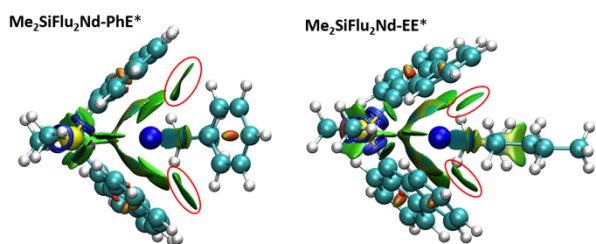


Figure 2 Non-covalent interaction analysis by reduced density gradient (NCI) plot of ethylene insertion transition states in a phenyl site ($\text{Me}_2\text{SiFlu}_2\text{Nd-PhE}^*$, left) and in alkyl site ($\text{Me}_2\text{SiFlu}_2\text{Nd-EE}^*$, right). The analysis has been implemented with cartesian coordinates. Steric interaction between phenyl or alkyl group and the ligand are encircled in red

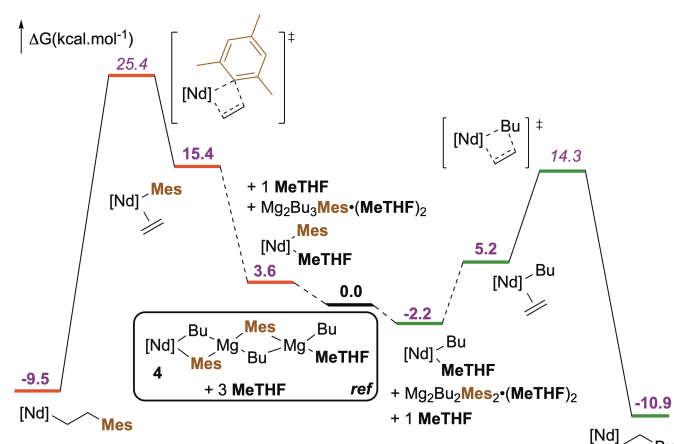


Figure 3 Gibbs free energy profile for the initiation step of ethylene insertion in alkyl site (green pathway) and phenyl site (red path) for the co-catalyst MesMgBu. Energies referring to kinetics are in italic and energies referring to thermodynamics are in bold. [Nd] correspond to $[(\text{Me}_2\text{Si}(\text{C}_{13}\text{H}_8)_2)\text{Nd}]$. ΔG in kcal.mol $^{-1}$ (B3PW91, TZVP, SMD (Toluene), D3BJ (SP))

The dissociation of complex **3** into a Nd-based complex and a Mg-based clusters yields either the solvated phenyl active site $[\text{Nd}]\text{Ph}(\text{MeTHF})$ (red pathway, Figure 1) or the solvated alkyl active site $[\text{Nd}]\text{Bu}(\text{MeTHF})$ (green pathway, Figure 1), upon alkyl / aryl exchange within **3**. After dissociation of MeTHF, ethylene can insert in the Nd-C bond of either the phenyl or the alkyl site thus initiating the polymerization. Relative to the heteropolymetallic complex **3**, ethylene insertion in the alkyl site is kinetically more favourable than the insertion in phenyl site by 3.8 kcal mol $^{-1}$ as indicated by the computed overall energy barriers 23.3 kcal mol $^{-1}$ vs 27.1 kcal mol $^{-1}$, respectively (Figure 1). Experimentally, initiation in the phenyl site has been evidenced, hence this Gibbs energy difference between the transition states is not large enough to ensure a selective initiation.

In order to further investigate the reactivity trend between the phenyl or alkyl sites towards ethylene insertion, the steric hindrance brought by the Ph and Bu groups within the monomer insertion transition states has been illustrated by means of a NCI analysis (Figure 2). Within transition states $\text{Me}_2\text{SiFlu}_2\text{Nd-PhE}^*$, weak interactions located out of the metallocene bisector plane, could be turned into more repulsive ones by adding substituent in the ortho position of the

phenyl ring. Such a modification would raise the energy barrier of initiation at the aryl site, thus increasing the chemoselectivity of the initiation. To test this hypothesis, the phenyl group has been conveniently replaced by a mesityl (2,4,6-trimethylphenyl, Mes) group. The chemoselectivity conferred to reaction by this aryl group was then assessed computationally.

First, the speciation of the newly designed co-catalyst has been performed (Figure S13). In this case, the most stable isomers are magnesium-based dimers in which two molecules of MeTHF bind each Mg centre: $(\text{MeTHF})(\sigma\text{-Mes})\text{Mg}(\mu\text{-Bu})(\mu\text{-Mes})\text{Mg}(\text{MeTHF})(\sigma\text{-Bu})$ and $(\text{MeTHF})(\sigma\text{-Bu})\text{Mg}(\mu\text{-Bu})(\mu\text{-Mes})\text{Mg}(\sigma\text{-MeTHF})(\sigma\text{-Bu})$. When associated to the neodymocene, the most stable complex is $\{(\text{Me}_2\text{Si}(\text{C}_{13}\text{H}_8)_2)\text{Nd}[(\mu\text{-nBu})(\mu\text{-Mes})\text{Mg}][(\mu\text{-nBu})(\mu\text{-Mes})\text{Mg}](\sigma\text{-Bu})\text{-MeTHF}\}$ (**4**). In presence of MeTHF, the most stable species is the coordinated active alkyl site. The formation of the mesityl active site is thermodynamically disfavoured due to the dissociation of the heterotrimetallic complex **4**. Concerning the reactivity towards ethylene, the insertion in the alkyl site shows an overall energy barrier of 16.5 kcal mol $^{-1}$ compared to the 27.6 kcal mol $^{-1}$ computed for the $[\text{Nd}]\text{-Mes}$ site (Figure 3). The reactivity trend is maintained with different functionals (see SI). Due to the significant difference of the overall monomer insertion energy barriers, the initiation of the polymerization should be specific enough on the alkyl site ethylene polymerization, at least. Based on this modelling investigation, the synthesis of the bis metalated CTA supporting two mesityl groups has been considered experimentally to assess its efficiency towards a selective initiation.

Synthesis of MesMg(CH $_2$) $_5$ MgMes and evaluation as CTA in polymerization. MesMg(CH $_2$) $_5$ MgMes (**2c**) was prepared by combining MeTHF solutions of **2b** and MesMgBr in 1/2 ratio. Dioxane was then added to shift the Schlenk equilibrium in favour of the formation of the symmetrical organomagnesium. After evaporation of the solvent, an oil was recovered and analyzed. **2c** was then solubilized in toluene at a concentration of 0.45 M (Scheme 1). The ^1H NMR analysis of the oil in C_6D_6 showed the characteristic signals for both mesityl and pentanediyl moieties (Figure 4). The integrals of the signals corresponding to the mesityl moieties and that of Mg-CH $_2$ at 0.12 ppm show a ratio of 1.87 instead of 2. The formation of a small percentage of the trimetallic species Mes{Mg(CH $_2$) $_5$ } $_2$ MgMes is assumed. This is confirmed by the presence of a triplet of low intensity is observed at -0.10 ppm. The integration of the signal of MeTHF gives a ratio MeTHF/Mg of 2.5. Note that some residual dioxane is observed in the ^1H NMR spectrum. **2c** was further characterized by 1D- ^{13}C NMR and 2D- $^1\text{H}/^1\text{H}$ COSY and NOESY and 2D- $^1\text{H}/^{13}\text{C}$ HMQC and HMBC (Figures S6 to S9). The NOESY analysis shows the proximity of the pentanediyl moiety with mesityl and MeTHF groups respectively. This agrees with the formation of the expected compound.

Ethylene was polymerized in the presence of **1** / **2c** catalytic system (Table 2, runs 4 and 5). A small fraction of the polymerization medium was deactivated with methanol.

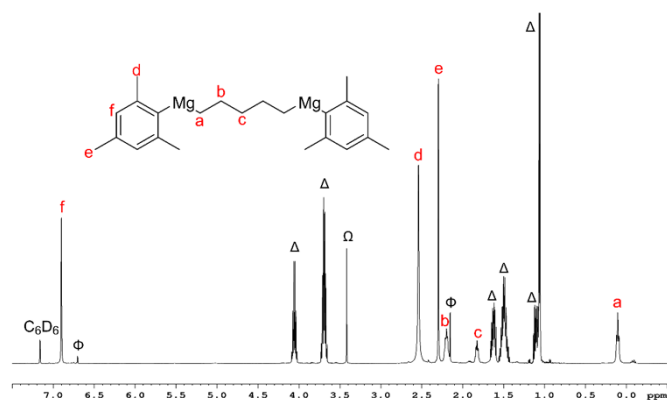


Figure 4 ^1H NMR in C_6D_6 at 298K of an aliquot of $\text{MesMg}(\text{CH}_2)_5\text{MgMes}$ (**2c**). Δ : MeTHF, Ω : dioxane and Φ : mesitylene

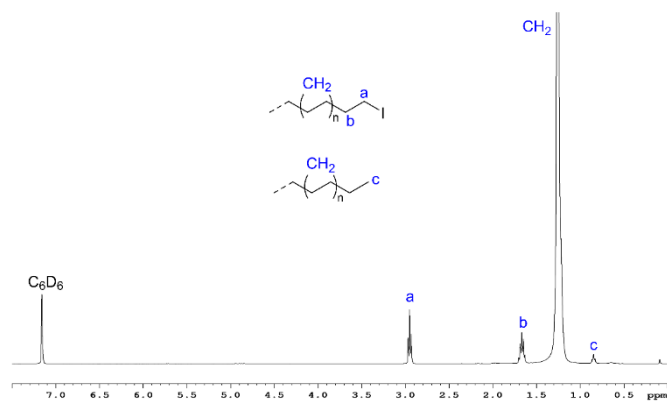


Figure 5 ^1H NMR in TCE/ C_6D_6 at 363K of the diiodo-polyethylene obtained with $\{(\text{Me}_2\text{Si}(\text{C}_{13}\text{H}_8)_2)\text{Nd}(\mu\text{-BH}_4)[(\mu\text{-BH}_4)\text{Li}(\text{THF})]_2\} / \text{2c}$ (Table 1, run 4)

Assuming initiation of one polymer chain per molecule of **2c**, experimental (1390 g mol^{-1}) and theoretical (1640 g mol^{-1}) M_n s are in good agreement and the molar mass distributions are narrow ($\mathcal{D} = 1.5$). In addition, the ^1H NMR spectra of the obtained polyethylene feature no signal in the aromatic region (Figure S10) and thus the absence of any imitation from the Mes moiety. These results fully validate the DFT predictions and the strategy of replacing of phenyl group by a mesityl group to selectively initiate all the chains from the alcanediyl moiety of the **2c** CTA. Telechelic polyethylenes should then be accessible for example by end capping the chains at the end of the polymerization by deactivation with iodine or deuterated methanol. The analysis of the ^1H NMR spectrum of the polyethylene obtained after deactivation with iodide shows the characteristic signal of iodo-terminated PE at 2.95 ppm (Figure 5).

Integrations of the signals of CH_2I and of the methyl chain showed an 87% functionalization of chain-ends. These results are in perfect agreement with our previous works on the end functionalization of PE chains using CCTP of ethylene with BOMAG⁴³ as CTA and the design of telechelic PE chains using bis(exoalkenyl) magnesium as CTA.¹⁹ In the case of the deactivation with MeOD, the determination of deuterated chain-end was performed by ^{13}C NMR analyses. The comparison of integrals of CH_3 and CH_2D show that 91% of chains are tagged with deuterium (Figure S11). These results and the successful use of **2c** in CCTP of ethylene consists in the first example of a

direct synthesis of telechelic polyethylene using a bis metalated - divalent alcanediyl magnesium compounds.

The catalytic system **1** / **2c** was then implemented in the copolymerization of ethylene with butadiene (Table 2, runs 7-9) and the results were compared with that obtained using **1**/BOMAG (Table 2, run 6). The analysis of the microstructure of the copolymers shows no influence of the nature of magnesium compound employed (Table 3, Figure S12) on the composition of the chains. If the activity is stable with time for BOMAG, **2c** leads to an increase in activity with polymerization time. In addition, the increase of the ratio $[\text{Mg}]/[\text{Nd}]$ is accompanied by a decrease in activity since longer polymerization times are required to reach the same yield. Interestingly, the molar masses decrease with the increase of $[\text{Mg}]/[\text{Nd}]$ ratio for the same polymer yield (Table 2, run 7-9). Moreover, there is a good agreement between theoretical and experimental molar masses and the dispersities remained low for all samples. This highlights the selective initiation of the copolymer chains from the divalent pentanediyl moiety and the efficiency of the CCTCoP induce by **2c**. The NMR analyses confirm the absence of any insertion in a neodymium mesityl bond.

Conclusions

In summary, this work reports an unprecedented selective divalent chain transfer agent for olefin polymerization. The new catalyst system $\{(\text{Me}_2\text{Si}(\text{C}_{13}\text{H}_8)_2)\text{Nd}(\mu\text{-BH}_4)[(\mu\text{-BH}_4)\text{Li}(\text{THF})]_2\} / \text{MesMg}(\text{CH}_2)_5\text{MgMes}$ is employed for the preparation of well-defined homotelechelic polyethylenes in one step and for controlled coordination copolymerization of ethylene with butadiene. This advances hold great promises for the design of block copolymers incorporating EBR segments and for new thermoplastic elastomers that will be discussed in future works.

Author Contributions

Project supervision, conceptualization – CB, FD, LP, FJBdD; Organometallic synthesis, polymerization experiments & characterizations – NB; Molecular Modelling – MNP, LV. Data analysis, Writing & Manuscript preparation – collective contributions from the authors.

Conflicts of interest

There are no conflicts to declare.

Acknowledgements

Manufacture Michelin is acknowledged for scientific and financial support of this project. M.N.P., L.V. and L.P. thank CCIR of ICBMS and P2CHPD of Université Lyon 1 for providing computational resources and technical support. N.B., F.D. and C.B. thank the NMR Polymer Center of Institut de Chimie de Lyon for access to the NMR facilities and assistance.

Notes and references

- D. Sauter, M. Taoufik and C. Boisson, *Polymers*, 2017, **9**, 185.
- G. Ricci, G. Pampaloni, A. Sommazzi and Francesco Masi, *Macromolecules*, 2021, **54**, 5879–5914.
- F. Barbotin, V. Monteil, M.-F. Llauro, C. Boisson and R. Spitz, *Macromolecules*, 2000, **33**, 8521–8523.
- P. Longo, S. Pragliola, G. Milano and G. Guerra, *J. Am. Chem. Soc.*, 2003, **125**, 4799–4803.
- P. Longo, M. Napoli, S. Pragliola, C. Costabile, G. Milano and G. Guerra, *Macromolecules*, 2003, **36**, 9067–9074.
- C. Boisson, V. Monteil, D. Ribour, R. Spitz and F. Barbotin, *Macromol. Chem. Phys.*, 2003, **204**, 1747–1754.
- J. Thuilliez, V. Monteil, R. Spitz and C. Boisson, *Angew. Chem. Int. Ed. Engl.*, 2005, **44**, 2593–2596.
- C. Capacchione, A. Avagliano and A. Proto, *Macromolecules*, 2008, **41**, 4573–4575.
- X. Li, M. Nishiura, L. Hu, K. Mori and Z. Hou, *J. Am. Chem. Soc.*, 2009, **131**, 13870–13882.
- H. Nsiri, I. Belaid, P. Larini, J. Thuilliez, C. Boisson and L. Perrin, *ACS Catal.*, 2016, **6**, 1028–1036.
- C. Wu, B. Liu, F. Lin, M. Wang and D. Cui, *Angew. Chem. Int. Ed. Engl.*, 2017, **56**, 6975–6979.
- L. Verrieux, J. Thuilliez, F. Jean-Baptiste-dit-Dominique, C. Boisson, M.-N. Poradowski and L. Perrin, *ACS Catal.*, 2020, **10**, 12359–12369.
- I. Belaid, V. Monteil and C. Boisson, Copolymerization of Ethylene with Conjugated Dienes. In *Handbook of Transition Metal Polymerization Catalysts*, 2nd ed.; Wiley: Hoboken, NJ, 2018; pp 661–692.
- J. Thuilliez, L. Ricard, F. Nief, F. Boisson and C. Boisson, *Macromolecules*, 2009, **42**, 3774–3779.
- I. Belaid, B. Macqueron, M.-N. Poradowski, S. Bouaouli, J. Thuilliez, F. Da Cruz-Boisson, V. Monteil, F. D'Agosto, L. Perrin and C. Boisson, *ACS Catalysis*, 2019, **9**, 9298–9309.
- J. Mazzolini, E. Espinosa, F. D'Agosto and C. Boisson, *Polym. Chem.*, 2010, **1**, 793–800.
- E. Altuntas, K. Kempe, A. Crecelius, R. Hoogenboom and U. S. Schubert, *Macromol. Chem. Phys.*, 2010, **211**, 2312–2322.
- T. S. Thomas, W. Hwang and L. R. Sita, *Angew. Chem. Int. Ed. Engl.*, 2016, **55**, 4683–4687.
- I. German, W. Kelhifi, S. Norsic, C. Boisson and F. D'Agosto, *Angew. Chem. Int. Ed. Engl.*, 2013, **52**, 3438–3441.
- H. Makio, T. Ochiai, J. Mohri, K. Takeda, T. Shimazaki, Y. Usui, S. Matsuura and T. Fujita, *J. Am. Chem. Soc.*, 2013, **135**, 8177–8180.
- D. J. Arriola, E. M. Carnahan, P. D. Hustad, R. L. Kuhlman and T. T. Wenzel, *Science*, 2006, **312**, 714–719.
- T. T. Wenzel, D. J. Arriola, E. M. Carnahan, P. D. Hustad and R. L. Kuhlman (2009) Chain Shuttling Catalysis and Olefin Block Copolymers (OBCs). In: Guan Z. (eds) *Metal Catalysts in Olefin Polymerization. Topics in Organometallic Chemistry*, vol 26. Springer, Berlin, Heidelberg.
- S. S. Park, C. S. Kim, S. D. Kim, S. J. Kwon, H. M. Lee, T. H. Kim, J. Y. Jeon and B. Y. Lee, *Macromolecules*, 2017, **50**, 6606–6616.
- S. D. Kim, T. J. Kim, S. J. Kwon, T. H. Kim, J. W. Baek, H. S. Park, H. J. Lee and B. Y. Lee, *Macromolecules*, 2018, **51**, 4821–4828.
- K. L. Park, J. W. Baek, S. H. Moon, S. M. Bae, J. C. Lee, J. Lee, M. S. Jeong and B. Y. Lee, *Polymers*, 2020, **12**, 1100.
- T. J. Kim, J. W. Baek, S. H. Moon, H. J. Lee, K. L. Park, S. M. Bae, J. C. Lee, P. C. Lee and B. Y. Lee, *Polymers*, 2020, **12**, 537.
- L. Sun, E. Szuromi, T. Karjala, Z. Zhou and E. Carnahan, *Macromolecules*, 2020, **53**, 10796–10802.
- V. Monteil, R. Spitz, F. Barbotin and C. Boisson, *Macromol. Chem. Phys.*, 2004, **205**, 737.
- A. D. Becke, *J. Chem. Phys.*, 1993, **98**, 5648–5652.
- J. P. Perdew and Y. Wang, *Phys. Rev. B*, 1992, **45**, 13244–13249.
- S. Grimme, J. Antony, S. Ehrlich and H. Krieg, *J. Chem. Phys.*, 2010, **132**, 154104.
- S. Grimme, S. Ehrlich and L. Goerigk, *J. Comput. Chem.*, 2011, **32**, 1456–1465.
- A. V. Marenich, C. J. Cramer and D. G. Truhlar, *J. Chem. Theory Comput.*, 2009, **5**, 2447–2464.
- R. Krishnan, J. Binkley, R. Seeger, J. Pople, *J. Chem. Phys.*, 1980, **72**, 650–654.
- T. Clark, J. Chandrasekhar, G. Spitznagel and P. Schleyer, *J. Comput. Chem.*, 1983, **4**, 294–301.
- A. Bergner, M. Dolg, W. Küchle, H. Stoll and H. Preuß, *Mol. Phys.*, 1993, **80**, 1431–1441.
- M. Dolg, H. Stoll, A. Savin and H. Preuß, *Theor. Chim. Acta*, 1989, **75**, 173–194.
- M. Dolg, H. Stoll, A. Savin and H. Preuß, *Theor. Chim. Acta*, 1993, **85**, 441–450.
- Gaussian 09, Revision D.01, M. J. Frisch, G. W. Trucks, H. B. Schlegel, G. E. Scuseria, M. A. Robb, J. R. Cheeseman, G. Scalmani, V. Barone, G. A. Petersson, H. Nakatsuji, X. Li, M. Caricato, A. Marenich, J. Bloino, B. G. Janesko, R. Gomperts, B. Mennucci, H. P. Hratchian, J. V. Ortiz, A. F. Izmaylov, J. L. Sonnenberg, D. Williams-Young, F. Ding, F. Lipparini, F. Egidi, J. Goings, B. Peng, A. Petrone, T. Henderson, D. Ranasinghe, V. G. Zakrzewski, J. Gao, N. Rega, G. Zheng, W. Liang, M. Hada, M. Ehara, K. Toyota, R. Fukuda, J. Hasegawa, M. Ishida, T. Nakajima, Y. Honda, O. Kitao, H. Nakai, T. Vreven, K. Throssell, J. A. Montgomery, Jr., J. E. Peralta, F. Ogliaro, M. Bearpark, J. J. Heyd, E. Brothers, K. N. Kudin, V. N. Staroverov, T. Keith, R. Kobayashi, J. Normand, K. Raghavachari, A. Rendell, J. C. Burant, S. S. Iyengar, J. Tomasi, M. Cossi, J. M. Millam, M. Klene, C. Adamo, R. Cammi, J. W. Ochterski, R. L. Martin, K. Morokuma, O. Farkas, J. B. Foresman and D. J. Fox, Gaussian, Inc., Wallingford CT, 2016.
- J. Contreras-García, E. R. Johnson, S. Keinan, R. Chaudret, J.-P. Piquemal, D. N. Beratan and W. Yang, *J. Chem. Theory Comput.*, 2011, **7**, 625–632.
- R. Ribeiro, R. Ruivo, H. Nsiri, S. Norsic, F. D'Agosto, L. Perrin, and C. Boisson, *ACS Catal.*, 2016, **6**, 851–860.
- E. Erdik and M. Koçoğlu, *J. Organomet. Chem.*, 2009, **694**, 1890–1897.
- R. Briquel, J. Mazzolini, T. Le Bris, O. Boyron, F. Boisson, F. Delolme, F. D'Agosto, C. Boisson and R. Spitz, *Angew. Chem. Int. Ed. Engl.*, 2008, **47**, 9311–9313.

Graphical abstract / TOC

